Structural versus Electrical Functionalization of Oligo(phenyleneethynylene) Diamine Molecular Junctions

M. Teresa González,[*,†] Xiaotao Zhao,[‡] David Zsolt Manrique,[¶] Delia Miguel,[§] Edmund Leary,[‖,†] Murat Gulcur,[‡] Andrei S. Batsanov,[‡] Gabino Rubio-Bollinger,[‖] Colin J. Lambert,[¶] Martin R. Bryce,[‡] and Nicolás Agraït[‖,†,⊥]

† *Instituto Madrileño de Estudios Avanzados en Nanociencia (IMDEA-Nanociencia), Ciudad Universitaria de Cantoblanco E-28049 Madrid, Spain,* ‡ *Department of Chemistry, Durham University, Durham DH1 3LE, United Kingdom,* ¶ *Department of Physics, Lancaster University, Lancaster LA1 4YB, England,* § *Departamento de Química Orgánica, Universidad de Granada, E-18071 Granada, Spain.,* ‖ *Departamento de Física de la Materia Condensada, Universidad Autónoma de Madrid, E-28049 Madrid, Spain, and* ⊥ *Instituto "Nicolás Cabrera", Universidad Autónoma de Madrid, E-28049, Madrid, Spain*

E-mail: teresa.gonzalez@imdea.org

[*]To whom correspondence should be addressed
[†]IMDEA-Nanociencia
[‡]Durham University
[¶]Lancaster University
[§]Universidad de Granada
[‖]Universidad Autónoma de Madrid
[⊥]Instituto Nicolás Cabrera

Abstract

We explore both experimentally and theoretically the conductance and packing of molecular junctions based on oligo(phenyleneethynylene) (OPE) diamine wires, when a series of functional groups are incorporated into the wires. Using the scanning tunnelling microscopy break junction (STM BJ) technique, we study these compounds in two environments (air and 1,2,4-trichlorobenzene) and explore different starting molecular concentrations. We show that the electrical conductance of the molecular junctions exhibit variations among different compounds, which are significant at standard concentrations but become unimportant when working at a low enough concentration. This shows that the main effect of the functional groups is to affect the packing of the molecular wires, rather than modifying their electrical properties. Our theoretical calculations consistently predict no significant changes in the conductance of the wires due to the electronic structure of the functional groups, although their ability to hinder ring rotations within the OPE backbone can lead to higher conductances at higher packing densities.

Introduction

Organic molecules can be tuned to achieve specific electronic functions, leading to the potential realisation of single-molecule diodes, rectifiers, memories, switches and thermoelectric devices.[1–4] Several techniques have been developed to characterize the electrical conductance of these nanoscale junctions, including conductive-probe atomic force microscopy (CP-AFM),[5,6] scanning tunneling microscopy break junctions (STM-BJs),[7,8] and mechanically controlled break junctions (MCBJs).[9–11]

During the last decade oligo(phenyleneethynylene) (OPE) derivatives have emerged as benchmark molecules for studying charge transport in molecular junctions. They are rigid, rod-like molecules with extended π-conjugation through the backbone and their functional properties can be systematically tuned by chemical synthesis.[12,13] In particular OPE3 systems (3 refers to the number of phenyl rings in the backbone) have been widely studied in metal−single-molecule−metal

junctions.[14–21]

For the purpose of designing future single-molecule devices, it is interesting to develop strategies for independently tuning electrical, mechanical and packing properties. In the present work, we demonstrate that this can be achieved by systematically varying the substituents on the central ring of gold-OPE3-gold junctions. The inclusion of lateral chemical groups is known to be a fruitful pathway for modifying the mechanical behavior of a molecule and developing a variety of active molecular devices.[22–27] The invariance of the junction conductance when a thiol-terminated OPE is functionalized on the central ring with alkoxy groups has been previously suggested.[18] In this paper, we put to the test the resilience of the electrical conductance of OPE3 by studying the effect of a range of functional groups on the central ring. We chose to work with weak amine binding groups, which we expect to play a less predominant role in the electron-transfer properties of the junctions than stronger binding groups.[28,29] Amines are also expected to provide a narrower spread of conductance values due to their more selective binding.[30] For a basic benzene unit, the effect on the molecular-junction conductance of substituting one or more hydrogen atoms by different functional groups has been previously explored.[29,31–35] Modest conductance variations have been reported for benzene-diamine[31] and benzene-dithiaalkane[32] molecular junctions. By studying the functionalization of the long OPE3 molecular wire, the functionalized region of the molecule is located further from the electrodes, thereby allowing us to separate intramolecular effects from interactions associated with the electrodes.

In addition to a possible effect on the electronic transmission of the compound, long substituent groups such as alkoxys are known to promote intermolecular interactions by chain interdigitation (see Hoeben et al[36] and references therein). This effect can promote junctions with a large number of wired molecules, which will subsequently display higher conductances. In order to separate steric from electronic effects, we performed experiments using different environments (air and 1,2,4-trichlorobenzene), as the environment has proved to be a relevant in some cases.[37–39] We also explored different concentrations of the molecule in solution, which is a parameter mostly overlooked for this kind of experiment.[40] We included in the study a compound with long alkyl

groups, for which we expect steric influence similar to that of alkoxy groups, but no significant effect on the energies and charge distributions of the OPE molecular orbitals.

We compare six OPE3 derivatives with functional groups varying from tetra-fluoro to tetra-methoxy groups, whose structures are shown in Figure 1. We perform our experimental studies using the scanning tunnelling microscopy break junction (STM BJ) technique. Our results show that changes in the concentration and the environment can produce significant variations on the profile of the resulting conductance histograms. We observed that these variations are stronger for some analogs, showing that, by systematically modifying the functional groups, we can successfully tune the molecular packing during molecular junction formation. Working at low enough concentrations we obtain practically the same histogram profile for the analogs, suggesting no direct effect of the functional group on the electrical properties of an individual OPE molecule at low bias voltage. We also present theoretical calculations which show that whenever the Fermi energy lies within the HOMO-LUMO gap, the effect of functional groups on the electrical transmission is expected to be practically negligible.

Methods

Synthesis

The OPE derivatives studied in this work are shown in Figure 1. In all cases, the synthetic strategy uses a two-fold Pd-catalyzed Sonogashira cross-coupling reaction of the corresponding diiodobenzene derivative with 4-ethynylaniline, following the literature precedent for the parent system OPE-4H.[41] The different substituents were chosen to provide systematic variation of the electronic and steric effects on the central ring: namely, strongly electron-donating methoxy and hexyloxy (OPE-2OC1; OPE-4OC1 and OPE-2OC6), weakly electron-donating octyl (OPE-2C8), and electron-withdrawing fluorine (OPE-4F). The hexyloxy and octyl substituents will have a similar steric effect, whereas the electron-donating effect of the former is greatly enhanced by the oxygen atoms attached to the benzene ring. Full details of the synthesis and characterization of

the new OPE derivatives are given in the Supporting Information. All the OPE derivatives were characterized by ^{1}H NMR, ^{13}C NMR and mass spectra which unambiguously confirmed their structures. Additionally, a single crystal X-ray structure was obtained for OPE-4F.

Break-junction experiments

We created our molecular junctions using the break-junction technique.[7] In particular, we worked with a home-built scanning tunneling microscope (STM), designed for high stability measurements, at room temperature, in air or liquid environments. We employed commercial gold substrates on quartz (Arrandee), which were cleaned in boiling ethanol, and flame-annealed with a butane flame. As STM tips, we used a 0.25 mm gold wire (99.99%), freshly cut before use. A liquid cell made of PEEK was fixed over the gold substrate with the help of a Kalrez o-ring, which assured the tightness of the cell. During the break-junction experiment, the tip moved vertically (with a 0.8 pm resolution) in and out of contact with the substrate to form and break gold contacts, during which time the conductance $G = I/V$ of the circuit was measured. A bias voltage V of 200 mV was maintained between the tip and the substrate, and a linear current-to-voltage converter with two amplification stages was used to measure the current I in the circuit. A 200 kΩ resistor, in-series with the substrate-tip circuit, prevented the current from extremely increasing when a thick gold contact is formed. This allowed us to verify that we reformed a gold contact in each break-junction cycle. Our gains in this work were 10^7 V/A after the first amplification stage, and 2×10^9 V/A after the second. These conditions allowed us to explore a range of conductance down to 5×10^{-7} G_0.

We performed experiments in two different environments: with the tip and substrate immersed in a solution of the respective compound in 1,2,4-trichlorobenzene (TCB); and in air, after immersing the substrate in a solution in dichloromethane (DCM) for several minutes and then drying it. We found that it was difficult to fully dry our substrates when using TCB as solvent due to its high boiling point (214° C, instead of 40° C for DCM). For this reason, we used DCM for the measurements in air.

Theoretical methods

At first, all the six OPE derivative molecules were constructed and geometrically relaxed as isolated molecules using the SIESTA[42] implementation of density functional theory (DFT). The PBE exchange-correlation functional was employed, with a double-zeta-polarized basis set and 0.01 eV/Å force tolerance. Next the relaxed molecules were placed symmetrically between two 35-atom gold 111 pyramids such that the distance between the apex gold atom and N-atom of the -NH_2 anchor group was 0.2 nm on both sides. These structures were again geometrically relaxed with SIESTA to obtain optimal junction geometries. During relaxation, the gold atoms were fixed. The resulting optimal junction configurations can be seen in Figure S19 in the supporting information. For the electron transport calculation, the gold pyramids were attached to wide-band leads with gold-gold coupling[43] from both sides and the transmission coefficients, $T(E)$ were calculated using the GOLLUM successor to the SMEAGOL package.[44,45]

Results and discussion

Conductance histograms

Using the STM break-junction technique, we studied the conductance of all the OPE analogs shown in Figure 1, both in TCB and in air. Typical examples of the individual G vs z traces recorded while moving the tip out of contact with the substrate can be seen in Figure 2 (a). We performed several experimental runs (changing to a new tip and substrate), with between 2000 and 5000 traces measured per run. Figure 2 (b) shows an example of the two-dimensional (2D) conductance histograms obtained after separating the traces with plateaus from those without plateaus.[46] Plateaus produced in the last stages of the gold nanocontacts generate the prominences at 1 G_0 and above ($z < 0$), while plateaus due to the formation of molecular junctions generate the prominences between $\log(G/G_0) = -5$ and -4 ($z > 0$).

Figure 3 (a) compares the one-dimensional histograms for all the OPE analogs obtained in air

after immersing a gold substrate into a standard 10^{-3} M DCM solution for several minutes. The percentage of the total number of measured traces that display plateaus, P_{tp}, is indicated close to each histogram. Figure 3 (a) shows that the profile of the histograms and the P_{tp} value can vary significantly between different analogs. The peaks of OPE-2OC6 and OPE-2OC1 (nomenclature specified in Figure 1) are broader and extend to lower conductance values, while that of OPE-2C8 appears centered at around half an order of magnitude higher conductance. The latter result was surprising, because C8 is electrically inert. We now demonstrate that this is a consequence of enhanced packing due to the presence of the C8 side groups. This enhancement is signalled by the large percentage of traces with plateaus (74 ± 8.4 %), which is significantly higher than for the rest of compounds (40-50 %). Considering that straight alkyl side chains favor the close-packing of molecules attached to the electrodes, a more compact molecular layer over the electrodes will increase the chances of trapping molecules (higher P_{tp}), and will favor junctions with more than one molecule attached to both electrodes, leading to a larger total conductance. It will in addition reduce ring rotations via steric hindrance, leading to an increase in the single-molecule conductance (see theory section below). Previous calculations have also shown that a higher single-molecule conductance is expected for diamines when they occupy also the surrounding preferred binding sites at the electrodes.[37]

In order to test our hypothesis, we repeated our experiments using a significantly lower concentration of OPE-2C8 in dichloromethane, and placing just a few drops over the substrate before drying under a N_2 flow. Figure 3 (b) shows the resulting histograms when starting with a 10^{-5} M solution (red, $P_{tp} = 44 \pm 9.3$ %) and with a 10^{-6} M solution (black, $P_{tp} = 33 \pm 9.8$ %). Indeed we see that by diminishing the number of available molecules to form junctions, both the percentage of traces with plateaus and the typical junction conductance are decreased. This result strongly supports the proposal that the C8 side group, rather than directly modifying the electrical properties of the OPE molecule, is changing its tendency to pack.

We found that the shape of the histogram of all the analogs changes when carrying out the experiments with 10^{-5} M concentration, although not to the same extent for all. Figure 4 (a) shows

that, by varying the molecular concentration, we can obtain peaks broadened towards low conductance values (see also Figure 3 (c)). This reflects the fact that a larger percentage of our traces display plateaus at low conductance values. Figures S10-S11 in the supporting information show that actually a second, less-defined, protuberance of the same length as the first is observed in the corresponding 2D-histograms, approximately located between $\log(G/G_0) = -5.5$ and -4.8. The observation of more than one conductance peak has been previously related to possible different configurations and binding geometries on the electrodes.[21,28,39,47,48] It is reasonable that when the number of molecules in the junctions is reduced, and therefore there are fewer constrains due to the interaction with other molecules, a larger number of configurations can occur. In addition, the relative rotation of the benzene rings can be blocked for closely-packed molecules, but can become more important when the molecules are dispersed. We show below in the theoretical section that the conductance of the OPE strongly decreases when the benzene rings rotate with respect to each other instead of being co-planar.

Figure 4 (b) shows the resulting histograms when the measurements are carried out in a 10^{-3} M TCB solution. The figure shows that the low-conductance broadening disappears for all the analogs, and the percentage of traces with plateaus increases. For OPE-2OC6, the histogram obtained using a 10^{-3} M solution (solid line in Figure 4 (b)) presents a peak centered on a significantly higher conductance than the rest, and only by reducing the TCB solution concentration to 10^{-5} M did we record a histogram similar to the other compounds (dashed line). This behavior is equivalent to that of OPE-2C8 measured in air from a DCM solution (see also Figure S13 of the supporting information). It seems reasonable that OPE-2OC6 and OPE-2C8, having the longest linear side chains, have an increased tendency to pack in parallel with the chains interdigitating when attached to gold.[36] Significantly we observed that this tendency is environment dependent, which probably reflects the different solubility of the compounds. OPE-2C8 being less polar than OPE-2OC6 should dissolve easier in TCB, which explains why it does not seem to pack as much as OPE-2OC6 in this solvent. The opposite happens when dissolving the compounds in DCM, which is a slightly more polar solvent than TCB.

The histograms in Figure 3 and reffig:His1Dconc show variations for a given compound when changing the experimental conditions, which are as large as the variation observed among the different compounds in Figure 3 (a). Importantly however we need to use a different sample preparation depending on the compound in order to obtain a particular histogram profile: while all measurements in air for OPE-2OC6 and OPE-2OC1 showed the low-conductance broadening, for OPE-4OC1 and OPE-4F we needed to decrease the initial solution concentration in DCM to 10^{-5} M, and for OPE-2C8 to 10^{-6} M. Also, as described above, for OPE-2C8 in air and OPE-2OC6 in TCB, when using a concentration of 10^{-5} M, we obtain similar results as for the other compounds, but for higher concentrations the results are drastically different. Our first conclusion from these results is that the functional groups modify significantly the sensitivity of the OPE to the environment and the sample preparation procedure. This fact has gone unnoticed in previous studies, and we consider it essential when drawing conclusions from comparisons between different species. A change in the chemical composition of a molecule can affect its packing and bonding properties without changing its electrical properties, but both types of change will influence the profile of the conductance histograms resulting from the break-junction experiment.

Comparison of conductance values

The described dependence of the percentage of traces with plateaus P_{tp} on concentration shows that P_{tp} is a good indicator of the local number of molecules close to the electrode apexes (see also Figure S14 in the supporting information). In order to investigate further the variations of the most probable conductance and P_{tp}, and how they correlate, we fitted a Gaussian to the conductance peaks as those of Figure 4, and identified $\log(G/G_0)_{mean}$ with its most-probable conductance. Figure 5 shows the dependence of $\log(G/G_0)_{mean}$ with P_{tp} along different experimental runs. Histograms that display a broadening towards low-conductance values (Figure 4 (a)) were better fitted by a sum of two Gaussians, whose corresponding two maxima are connected by a dashed line in Figure 5. Examples of these fits can be seen in the supporting information (Figure S15). The figure shows that low conductance peaks are only clearly observed for percentages of traces with

plateaus below 40 %, while the maximum of the upper conductance peak slightly increases with P_{tp}. In addition, we see that performing the experiment in TCB (solid symbols) favors the binding of molecules to the electrodes compared to the measurements in air (open and cross symbols), as higher P_{tp} values were normally observed. We note here that this is in contrast with the results for acetyl-protected OPE-dithiols.[20] In that case, to dry the sample helped the deprotection of the thiols resulting in higher P_{tp} values in air than in TCB. We calculated also the plateau-length distributions for all the OPE derivatives in different experimental runs (Figure S16), and found that, for a given environment, the plateau length increases linearly with P_{tp}, which is consistent with the idea of having a larger number of molecules in the junction.[49,50]

For the measurements in TCB (solid symbols), we included the results of two experimental runs for each compound in Figure 5. Apart from the case of OPE-2OC6 discussed above, these two results were obtained under the same experimental conditions (10^{-3} M TCB solution) illustrating that the junction formation probability P_{tp} can vary significantly between runs, which will translate also in a conductance variation (comparisons between whole resulting histograms are shown in Figure S17). This variability of P_{tp} reflects the fact that the local concentration of molecules around the electrodes can at best be only partially controlled externally in a break-junction experiment, as can the topography of the electrodes[40,51] and the local presence of ambient impurities. All these factors affect how likely it is for the molecules to adopt a given configuration between the electrodes, or to pack and form multi-molecule junctions. These are not random variations that change from trace to trace, but factors that influence the measurements over many traces. This introduces a dispersion in any result of the break-junction experiment, that is most important when comparing conductance values for different compounds. For OPE-diamines, we estimate this dispersion in around 0.25 in the logarithm of the conductance (around a factor 2 in linear scale).

Having discussed and eliminated the influence of the environment and packing, we conclude from Figure 5 that there is no clear dependence of the conductance values with the functional group. Most of the $\log(G/G_0)_{mean}$ values for the high conductance peak are within the averaged interval -4.35 ± 0.12 (indicated by horizontal lines in Figure 5). Additionally, by combining all

the results recorded in an environment in a single histogram (Figure S18 in the supporting information), we observed that the conductance variation among compounds follows a different trend in air and in TCB, and none of these trends follows the calculated ionization potential as reported for benzene diamine.[31] More importantly, the conductance differences between compounds are within the same dispersion interval of 0.25 observed among different measurements for a given compound. From this we conclude that the conductance variations introduced by the functional groups in OPE molecular junctions are related to their different packing and sensitivity to the environment, rather than by a direct effect of the functional group on the electrical transmission of a OPE-diamine.

Theoretical calculations

Figure 6(a) shows the theoretical transmission coefficients $T(E)$ for the relaxed molecules (see Figure S19 in the supporting information), which yield their electrical conductances G via the Landauer formula $G = G_0 \times T(E_F)$, where G_0 is the quantum of conductance. Figure 6(a) clearly shows that the transmission coefficients at $E = E_F$ are very similar for all compounds and therefore the predicted single-molecule conductances are insensitive to functionalization, even though the HOMO and LUMO resonances are shifted compared to OPE-4H. The estimated conductance value for OPE-2OC6 and OPE-2OC1 is slightly larger than that of the rest of the compounds. This apparently is an indirect influence of the anti-resonances around -1.4 eV, which push the HOMO level closer to the Fermi energy, reducing the HOMO-LUMO gap and increasing the conductance. Anti-resonances of this type are a known feature of molecules with pendant oxygens.[52–55] The computed conductance value is sensitive to the position of the Fermi energy relative to the resonances, which may vary with the electrode separation and junction geometry and therefore cannot be calculated with certainty. Theoretically we find that the transmission coefficients in the presence of functional groups take the same values at an energy of approximately 0.3 eV above the DFT-predicted value of E_F. Our low-concentration experimental observation, that all compounds have approximately the same conductance is therefore consistent with theory, provided the func-

tional groups do not influence the relative Fermi energy position and that E_F lies 0.3 eV above the DFT-predicted value.

The above results predict conductance values significantly higher than those experimentally observed, which is partly attributed to the neglected screening effects in DFT.[56] However these results were computed for molecules with co-planar rings. At high packing densities, ring rotations will be sterically hindered. However at lower densities, there is a low barrier to rotation and the central ring of the OPE backbone is expected to randomly sample all angles of twist, leading to an entropic contribution to the conductance. Figure 6(b) shows the twist angle dependence of the conductance and clearly demonstrates major conductance reductions as expected.[57] The dashed horizontal line shows the conductance G/G_0 obtained by averaging over all twist angles and demonstrates that the inclusion of rotational entropy reduces the conductance by a factor of 0.25. Examples of transmission curves for all molecules in the presence of twist are presented in the supporting information (Figure S20). The slight differences in their response to twist suggests that rotational is as important as the electronic structure in producing the slight differences in conductance between the compounds of Figure 1 and in particular to the decrease in conductance with decreasing concentration, shown in Figure 3 (b) and (c).

Conclusions

We have compared experimentally and theoretically the properties of molecular junctions formed by six OPE-diamine derivatives with different functional groups. Changing the concentration of the OPE derivatives in our measurements, we have observed significant variations in the histogram profiles and junction formation probabilities of all compounds. These variations reflect the difference between having dispersed, non-interacting, molecules attached to the electrodes, or closely-packed and interacting molecules. We found that the solution concentration needed to observe these two behaviors is different for different analogs, implying that the packing of the OPE molecular wire can be tuned by modifying the functional group. We observed in addition that this packing effect

is solvent dependent for some functional groups. On the other hand, the conductance variations observed between different analogs are smaller than those for any one molecule when changing the local concentration (typically of a quarter of an order of magnitude in conductance), which highlights the resilience of the electrical conductance of OPEs to lateral functionalization. This is in agreement with our theoretical calculations that predict very little effect of the functional groups on the electrical conductance of single molecules in vacuum. However steric hindrance at higher concentrations will reduce ring rotations within the OPE backbone, leading to a predicted increase in single-molecule conductance with increasing concentration. Our results demonstrate the importance of taking into account packing, steric hindrance and other concentration and solvent effects when comparing break-junction results of compounds with different compositions. In addition, they suggest that, by laterally adding functional groups, we can favor the self-assembly of OPE molecules, without substantially affecting electrical transport properties, which is attractive for the design of more complex molecular architectures.

Acknowledgement

This work was supported by the Spanish Ministerio de Economía y Competitividad through the projects MAT2011-25046, RYC-2008-03328, and CSD2007-0010 (Consolider-ingenio, nanociencia molecular), the CAM through the project S2009/MAT-1726 (Nanobiomagnet), the UK EPSRC and the EU through the FP7 ITNs MOLESCO and FUNMOLS (project numbers 606728 and 212942, respectively) and ELFOS (FP7-ICT2009-6). X.Z. thanks the China Scholarship Council for a studentship award.

Supporting Information Available

Details of molecular synthesis and characterization; X-ray crystallographic data for OPE-4F (CCDC 968033); UV-vis spectra of all the analogs; 2D-histograms for all the studied analogs obtained both in air from a DCM solution and in TCB, using a standard 10^{-3} M concentration; Comparison of the 2D-histograms obtained in air when lower concentrations are used; Variation of the probability of

observing plateaus with the concentration; Examples of the resulting fits of Gassians to the peaks in the conductance histograms; Mean plateau lengths for all the OPE derivatives from different experimental runs and in different experimental conditions; Mean conductance values for all the compounds both in air and in TCB; Geometrically relaxed junction configurations; and transmission functions for the molecules with twisted inner aromatic ring. This material is available free of charge via the Internet at http://pubs.acs.org.

References

(1) Weibel, N.; Grunder, S.; Mayor, M. *Org. Biomol. Chem.* **2007**, *5*, 2343–2353.

(2) van der Molen, S. J.; Liljeroth, P. *J. Phys.: Condens. Matter* **2010**, *22*, 133001/1–30.

(3) Aradhya, S. V.; Venkataraman, L. *Nature Nanotech.* **2013**, *8*, 399–410.

(4) Malen, J. A.; Yee, S. K.; Majumdar, A.; Segalman, R. A. *Chem. Phys. Lett.* **2010**, *491*, 109–122.

(5) Cui, X.; Primak, A.; Zarate, X.; Tomfohr, J.; Sankey, O.; Moore, A.; Moore, T.; Gust, D.; Harris, G.; Lindsay, S. *Science* **2001**, *294*, 571–574.

(6) Fan, F.; Yang, J.; Cai, L.; Price, D.; Dirk, S.; Kosynkin, D.; Yao, Y.; Rawlett, A.; Tour, J.; Bard, A. *J. Am. Chem. Soc.* **2002**, *124*, 5550–5560.

(7) Xu, B.; Tao, N. *Science* **2003**, *301*, 1221–1223.

(8) Haiss, W.; Nichols, R.; van Zalinge, H.; Higgins, S.; Bethell, D.; Schiffrin, D. *Phys. Chem. Chem. Phys.* **2004**, *6*, 4330–4337.

(9) Reed, M. A.; Zhou, C.; Muller, C. J.; Burgin, T. P.; Tour, J. M. *Science* **1997**, *278*, 252–254.

(10) Smit, R.; Noat, Y.; Untiedt, C.; Lang, N.; van Hemert, M.; van Ruitenbeek, J. *Nature* **2002**, *419*, 906–909.

(11) Wu, S.; Gonzalez, M. T.; Huber, R.; Grunder, S.; Mayor, M.; Schoenenberger, C.; Calame, M. *Nature Nanotechnol.* **2008**, *3*, 569–574.

(12) Bunz, U. *Chem. Rev.* **2000**, *100*, 1605–1644.

(13) Jenny, N. M.; Mayor, M.; Eaton, T. R. *Eur. J. Org. Chem.* **2011**, 4965–4983.

(14) Tour, J.; Rawlett, A.; Kozaki, M.; Yao, Y.; Jagessar, R.; Dirk, S.; Price, D.; Reed, M.; Zhou, C.; Chen, J.; et al., *Chem. Eur. J.* **2001**, *7*, 5118–5134.

(15) James, D.; Tour, J. *Chem. Mater.* **2004**, *16*, 4423–4435.

(16) Blum, A. S.; Kushmerick, J.; Long, D.; Patterson, C.; Yang, J.; Henderson, J.; Yao, Y.; Tour, J.; Shashidhar, R.; Ratna, B. *Nature Materials* **2005**, *4*, 167–172.

(17) Liao, J.; Bernard, L.; Langer, M.; Schonenberger, C.; Calame, M. *Adv. Mater.* **2006**, *18*, 2444–2447.

(18) Huber, R.; Gonzalez, M. T.; Wu, S.; Langer, M.; Grunder, S.; Horhoiu, V.; Mayor, M.; Bryce, M. R.; Wang, C.; Jitchati, R.; et al., *J. Am. Chem. Soc.* **2008**, *130*, 1080–1084.

(19) Lu, Q.; Liu, K.; Zhang, H.; Du, Z.; Wang, X.; Wang, F. *ACS Nano* **2009**, *3*, 3861–3868.

(20) Gonzalez, M. T.; Leary, E.; Garcia, R.; Verma, P.; Herranz, M. A.; Rubio-Bollinger, G.; Martin, N.; Agrait, N. *J. Phys. Chem. C* **2011**, *115*, 17973–17978.

(21) Kaliginedi, V.; Moreno-Garcia, P.; Valkenier, H.; Hong, W.; Garcia-Suarez, V. M.; Buiter, P.; Otten, J. L. H.; Hummelen, J. C.; Lambert, C. J.; Wandlowski, T. *J. Am. Chem. Soc.* **2012**, *134*, 5262–5275.

(22) Reichert, J.; Ochs, R.; Beckmann, D.; Weber, H.; Mayor, M.; von Lohneysen, H. *Phys. Rev. Lett.* **2002**, *88*, 176804/1–4.

(23) Xiao, X.; Nagahara, L.; Rawlett, A.; Tao, N. *J. Am. Chem. Soc.* **2005**, *127*, 9235–9240.

(24) Wang, C.; Batsanov, A.; Bryce, M.; Ashwell, G.; Urasinska, B.; Grace, I.; Lambert, C. *Nanotechnology* **2007**, *18*, 044005/1–8.

(25) Grunder, S.; Huber, R.; Horhoiu, V.; Gonzalez, M. T.; Schoenenberger, C.; Calame, M.; Mayor, M. *J. Org. Chem.* **2007**, *72*, 8337–8344.

(26) Grunder, S.; Huber, R.; Wu, S.; Schoenenberger, C.; Calame, M.; Mayor, M. *Eur. J. Org. Chem.* **2010**, 833–845.

(27) Weibel, N.; Blaszczyk, A.; von Haenisch, C.; Mayor, M.; Pobelov, I.; Wandlowski, T.; Chen, F.; Tao, N. *Eur. J. Org. Chem.* **2008**, 136–149.

(28) Li, C.; Pobelov, I.; Wandlowski, T.; Bagrets, A.; Arnold, A.; Evers, F. *J. Am. Chem. Soc.* **2008**, *130*, 318–326.

(29) Chen, W.; Widawsky, J. R.; Vazquez, H.; Schneebeli, S. T.; Hybertsen, M. S.; Breslow, R.; Venkataraman, L. *J. Am. Chem. Soc.* **2011**, *133*, 17160–17163.

(30) Venkataraman, L.; Klare, J. E.; Tam, I. W.; Nuckolls, C.; Hybertsen, M. S.; Steigerwald, M. L. *Nano Lett.* **2006**, *6*, 458–462.

(31) Venkataraman, L.; Park, Y. S.; Whalley, A. C.; Nuckolls, C.; Hybertsen, M. S.; Steigerwald, M. L. *Nano Lett.* **2007**, *7*, 502–506.

(32) Leary, E.; Higgins, S. J.; van Zalinge, H.; Haiss, W.; Nichols, R. J. *Chem. Commun.* **2007**, 3939–3941.

(33) Mowbray, D. J.; Jones, G.; Thygesen, K. S. *J. Chem. Phys.* **2008**, *128*, 111103/1–5.

(34) Dell'Angela, M.; Kladnik, G.; Cossaro, A.; Verdini, A.; Kamenetska, M.; Tamblyn, I.; Quek, S. Y.; Neaton, J. B.; Cvetko, D.; Morgante, A.; et al., *Nano Lett.* **2010**, *10*, 2470–2474.

(35) Bilan, S.; Zotti, L. A.; Pauly, F.; Cuevas, J. C. *Phys. Rev. B* **2012**, *85*, 205403/1–9.

(36) Hoeben, F.; Jonkheijm, P.; Meijer, E.; Schenning, A. *Chem. Rev.* **2005**, *105*, 1491–1546.

(37) Fatemi, V.; Kamenetska, M.; Neaton, J. B.; Venkataraman, L. *Nano Lett.* **2011**, *11*, 1988–1992.

(38) Leary, E.; Hobenreich, H.; Higgins, S. J.; van Zalinge, H.; Haiss, W.; Nichols, R. J.; Finch, C. M.; Grace, I.; Lambert, C. J.; McGrath, R.; et al., *Phys. Rev. Lett.* **2009**, *102*, 086801/1–4.

(39) Li, X.; He, J.; Hihath, J.; Xu, B.; Lindsay, S. M.; Tao, N. *J. Am. Chem. Soc.* **2006**, *128*, 2135–2141.

(40) French, W. R.; Iacovella, C. R.; Cummings, P. T. *ACS Nano* **2012**, *6*, 2779–2789.

(41) Sonogashira, K. *J. Organomet. Chem.* **2002**, *653*, 46–49.

(42) Soler, J. M.; Artacho, E.; Gale, J. D.; García, A.; Junquera, J.; Ordejón, P.; Sánchez-Portal, D. *J. Phys.: Condens. Matter* **2002**, *14*, 2745–2799.

(43) Verzijl, C. J. O.; Seldenthuis, J. S.; Thijssen, J. M. *J. Chem. Phys.* **2013**, *138*, 094102/1–10.

(44) Rocha, A. R.; Garcia-Suarez, V. M.; Bailey, S. W.; Lambert, C. J.; Ferrer, J.; Sanvito, S. *Nature Materials* **2005**, *4*, 335–339.

(45) Rocha, A. R.; García-Suárez, V. M.; Bailey, S.; Lambert, C.; Ferrer, J.; Sanvito, S. *Phys. Rev. B* **2006**, *73*, 085414/1–22.

(46) As previously described,[20,49] we consider that a trace has a plateau whenever an elongation Δz larger than 0.1 nm is needed to produce a decay in conductance of $\Delta \log(G/G_0) = 0.1$ at any conductance below 0.5 G_0. Examples of the histograms before trace separation for OPE-4H have been previously published.[50]The histograms were built after aligning all the traces on the z-axis just after the breaking of the gold contact ($z = 0$), and using bin sizes of $\Delta \log(G/G_0) = 0.03$ and $\Delta z = 0.03$ nm.

(47) Moreno-Garcia, P.; Gulcur, M.; Manrique, D. Z.; Pope, T.; Hong, W.; Kaliginedi, V.; Huang, C.; Batsanov, A. S.; Bryce, M. R.; Lambert, C.; et al., *J. Am. Chem. Soc.* **2013**, *135*, 12228–12240.

(48) Alexis Paz, S.; Zoloff Michoff, M. E.; Negre, C. F. A.; Olmos-Asar, J. A.; Mariscal, M. M.; Sanchez, C. G.; Leiva, E. P. M. *Phys. Chem. Chem. Phys.* **2013**, *15*, 1526–1531.

(49) Arroyo, C. R.; Leary, E.; Castellanos-Gomez, A.; Rubio-Bollinger, G.; Gonzalez, M. T.; Agrait, N. *J. Am. Chem. Soc.* **2011**, *133*, 14313–14319.

(50) Gonzalez, M. T.; Diaz, A.; Leary, E.; Garcia, R.; Herranz, M. A.; Rubio-Bollinger, G.; Martin, N.; Agrait, N. *J. Am. Chem. Soc.* **2013**, *135*, 5420–5426.

(51) Haiss, W.; Martin, S.; Leary, E.; van Zalinge, H.; Higgins, S. J.; Bouffier, L.; Nichols, R. J. *J. Phys. Chem. C* **2009**, *113*, 5823–5833.

(52) Papadopoulos, T.; Grace, I.; Lambert, C. *Phys. Rev. B* **2006**, *74*, 193306/1–4.

(53) Wang, C.; Bryce, M. R.; Gigon, J.; Ashwell, G. J.; Grace, I.; Lambert, C. J. *J. Org. Chem.* **2008**, *73*, 4810–4818.

(54) Bergfield, J. P.; Solis, M. A.; Stafford, C. A. *ACS Nano* **2010**, *4*, 5314–5320.

(55) Ricks, A. B.; Solomon, G. C.; Colvin, M. T.; Scott, A. M.; Chen, K.; Ratner, M. A.; Wasielewski, M. R. *J. Am. Chem. Soc.* **2010**, *132*, 15427–15434.

(56) Jin, C.; Strange, M.; Markussen, T.; Solomon, T. K. S., G. C. *J. Chem. Phys.* **2013**, *139*, 184307/1–6.

(57) Venkataraman, L.; Klare, J. E.; Nuckolls, C.; Hybertsen, M. S.; Steigerwald, M. L. *Nature* **2006**, *442*, 904–907.

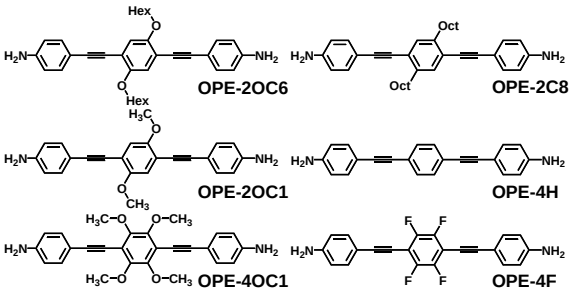

Figure 1: Schematics of all the compounds studied in this work. We specify here the nomenclature used throughout the article.

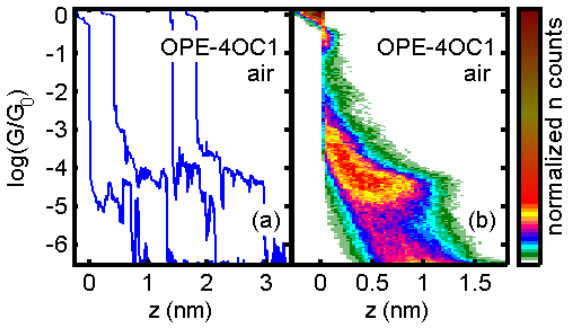

Figure 2: (a) Examples of individual G vs z traces showing plateaus for OPE-4OC1 recorded in air. (b) Corresponding two-dimensional histogram built with more than 2000 traces as those in part (a).

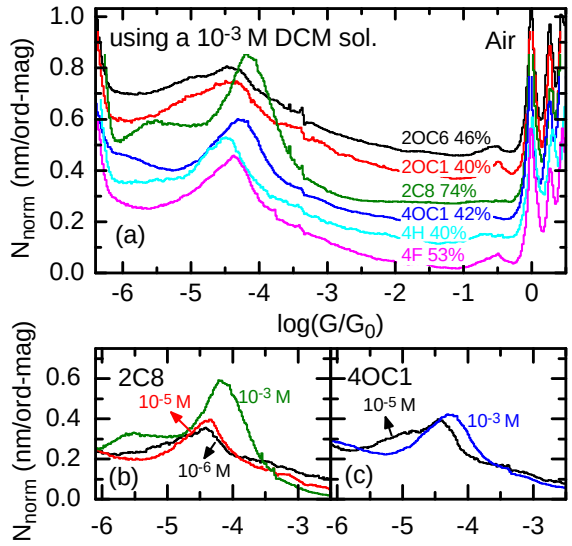

Figure 3: (a) One-dimensional log G-histograms for all the studied compounds deposited from a 10^{-3} M DCM solution and measured in air (shifted vertically for clarity). In all cases the histograms were built from those G vs z traces presenting plateaus.[46] The percentage of those with respect to total number of recorded traces is written close to each histogram. (b)-(c) Histograms obtained in air using different initial solution concentrations for OPE-2C8 and OPE-4OC1.

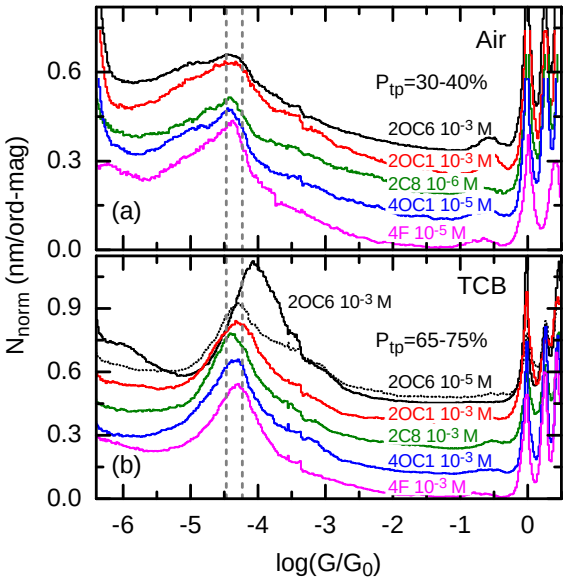

Figure 4: Comparison of histograms obtained at a similar percentage of traces with plateaus P_{tp} in air (a) and TCB (b). These histograms were obtained using various solution concentrations depending on the compound. The histograms obtained at similar P_{tp} are quite alike. Those corresponding to a P_{tp}=30-40 % all show a shoulder towards low conductance values, while, in those corresponding to P_{tp}=65-75 %, the shoulder is completely absent. The vertical dashed lines indicate the range where most of the peak maxima were observed.

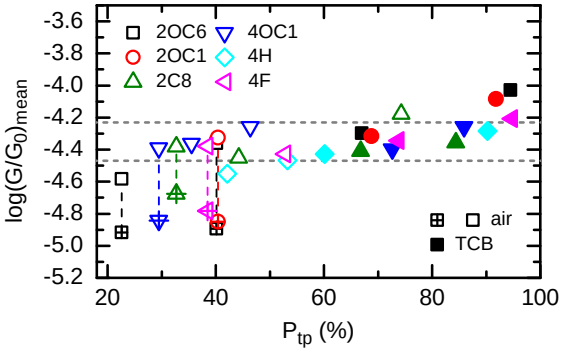

Figure 5: (a) Correlation between the percentage of traces with plateaus P_{tp} and the peak maxima in the conductance histograms, along different runs for all the studied compounds. The points connected by a dashed line correspond to the same histogram whose profile has been fitted by a sum of two Gaussians (see text for details).

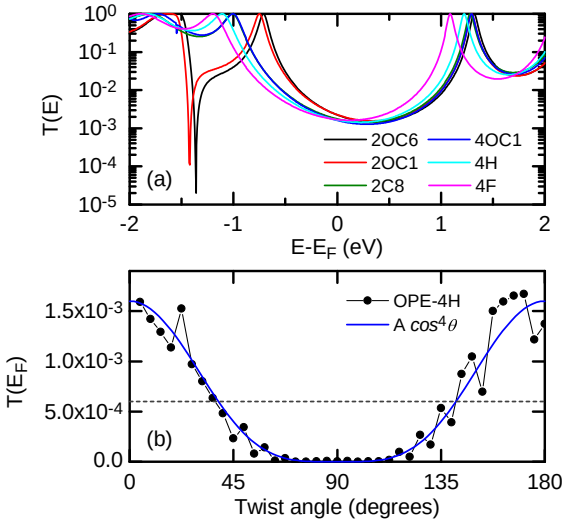

Figure 6: (a) Transmission coefficient functions for the six OPE analogs. It is remarkable that in all cases the estimated conductance values, calculated by the Landauer formula, $G = G_0 \times T(E_F)$ with various choices of Fermi energy, are very similar. (b) Calculated conductance as a function of twist angle of the central aromatic ring for the OPE-4H molecule. The horizontal dashed line is the numerical average conductance. The blue line is a fitted $cos^4\theta$ curve. In the calculations the outer aromatic rings in the molecule are aligned parallel to each other (see Figure S21 in the supporting information).

Table of Contents (TOC) Graphic